Microbiological Research 263 (2022) 127132

Contents lists available at ScienceDirect

Microbiological Research

journal homepage: www.elsevier.com/locate/micres

Study of the influence of fecal material on the prognosis of intra-abdominal candidiasis using a murine model of technetium-99 m (^{99m}Tc)-*Candida albicans*

William Gustavo Lima [a,*,1,2], Aline Beatriz do Couto Campos [a,1], Júlio César Moreira Brito [b,3], Valbert Nascimento Cardoso [a,4], Simone Odília Antunes Fernandes [a,*,5]

[a] *Laboratório de radioisótopos, Departamento de Análises Clínicas, Faculdade de Farmácia, Universidade Federal de Minas Gerais, Belo Horizonte, MG, Brazil*
[b] *Fundação Ezequiel Dias (FUNED), Belo Horizonte, MG, Brazil*

ARTICLE INFO

Keywords:
Candida albicans
Radiolabeling
Technetium-99 m
Peritonitis
Abscess

ABSTRACT

Intra-abdominal candidiasis (IAC) occurs due to the direct inoculation of *Candida* into the sterile peritoneal cavity or leakage of the gastrointestinal tract. An important difference between the two forms of the disease is the presence of fecal material, which is exclusive to the latter condition. However, the influence of fecal material on the prognosis of IAC is still poorly understood. Furthermore, methodologies that use the quantification of fungal load by culture methods have low sensitivity, as they do not adequately show the precocity of the infectious process. Here, we developed a new method to evaluate the aspects of the pathophysiology of IAC, mainly the influence of fecal material on the prognosis of infection, by using *C. albicans* radiolabeled with technetium-99 m (^{99m}Tc). *C. albicans* was successfully radiolabeled with ^{99m}Tc (18.5 MBq) using dihydrate stannous chloride (100 μM) as a reducing agent. This binding was stable for 72 h. Viability, yeast-to-hyphae transition, morphology, and antifungal susceptibility were not altered by radiolabeling *C. albicans* with ^{99m}Tc. The biomass and the fungal load of ^{99m}Tc-*C. albicans* biofilms were reduced compared to the *C. albicans* non-radiolabeled after 72 h and 48 h of incubation, respectively. In the IAC model, the fungal load in the biodistribution of ^{99m}Tc-*C. albicans* and culture assays was higher in animals receiving fungal inoculum without fecal material, suggesting that the presence of this component reduces the invasiveness of the pathogen.

1. Introduction

Candidiasis is a disease caused by different species of the genus *Candida* that can manifest as a generally self-limiting superficial infection (e.g., oral and vulvovaginal candidiasis) (Millsop and Fazel, 2016; Sobel, 2007; Ghorbani et al., 2018; Fakhim et al., 2020) or as a life-threatening invasive infection (Schmiedel and Zimmerli, 2016). Invasive candidiasis can be divided into candidemia and deep-seated candidiasis (Centers for Disease Control and Prevention, 2020), in which intra-abdominal candidiasis (IAC) is the most common form of deep-seated candidiasis (Azim et al., 2017; Vergidis et al., 2016). IAC usually occurs due to direct inoculation of *Candida* into the sterile peritoneal cavity, caused by, for example, infected peritoneal dialysis catheters or, more commonly, as a result of leakage or perforation of the gastrointestinal tract (Azim et al., 2017). The course of IAC is associated with peritonitis as a result of the host's response to *Candida* in the peritoneal cavity, followed by abscess formation, which occurs in the following days. During abscess formation, *Candida* cells invading the abdominal organs from the peritoneal cavity are contained, walled off, and eventually eliminated by the inflammatory response (Montravers et al., 2013). When the immune response associated with abscess formation cannot control the infection, the pathogen spreads into the

* Corresponding authors.
E-mail addresses: williamlimainfecto@gmail.com (W.G. Lima), simoneodilia@yahoo.com.br (S.O.A. Fernandes).
[1] These authors also contributed to this article
[2] 0000-0001-8946-9363
[3] ORCID: 0000-0003-2794-5680
[4] 0000-0001-7597-9602
[5] ORCID: 0000-0002-6139-5187

https://doi.org/10.1016/j.micres.2022.127132
Received 27 April 2022; Received in revised form 11 July 2022; Accepted 13 July 2022
Available online 22 July 2022

bloodstream and causes candidemia (Vergidis et al., 2016).

Peritonitis in IAC can be primary, occurring in patients with no apparent break in the gastrointestinal epithelial continuity (e.g., peritonitis due to dialysis catheter), or secondary, occurring in patients with a break in the gastrointestinal continuity resulting in contamination of the abdominal cavity with gastrointestinal contents (e.g., after accidents or surgery) (Azim et al., 2017). The main difference between the two forms of peritonitis observed in IAC is the presence of fecal material, which is exclusive to secondary peritonitis. However, little is known about whether the presence of fecal material can influence the severity of *Candida* infection (Andrade et al., 2021; Lima et al., 2019, 2022). Furthermore, despite the clinical importance of IAC, its pathogenesis has not been well elucidated. Mouse models of IAC have been developed, but they have not been widely used to study the full spectrum of infection and have limitations in determining the fungal boundary after peritoneal infection (Cheng et al., 2013). The most commonly used method for quantifying fungal burden in mice tissues is based on plating and counting colonies on Sabouraud-dextrose agar, which is not suitable for accurate detection and quantification of fungal burden at early stages of infection (Costa et al., 2018).

In this context, nuclear techniques are a promising tool for assessing fungal infections, especially in the early stages of the disease. Several groups have successfully radiolabeled bacteria of medical interest, such as *Escherichia coli* (Diniz et al., 1999; Eaves-Pyles et al., 2000), *Staphylococcus aureus* (Ardehali and Mohammad, 1993), *Staphylococcus epidermidis* (Ardehali and Mohammad, 1993), and *Pseudomonas aeruginosa* (Ardehali and Mohammad, 1993) and used these microorganisms as models to study various aspects of the host-parasite relationship. In most studies, technetium-99 m was used as a radionuclide since it has ideal physicochemical properties for labeling and use in biological systems (Kane and Davis, 2021). Indeed, $^{99\ m}$Tc is very versatile as it can react with various molecules and produce scintigraphy images of high sensitivity (Andrade et al., 2021; Diniz et al., 2005; Kane and Davis, 2021).

Despite the advantages of nuclear techniques in the study of infectious diseases, to the best of our knowledge, there is only one study that used this methodology to investigate fungal infections (Costa et al., 2018). Costa et al. (2018) efficiently radiolabeled cells of *Cryptococcus gatti* with $^{99\ m}$Tc without affecting the viability of the pathogen. Interestingly, the use of $^{99\ m}$Tc-*C. gattii* allowed the assessment of brain tissue invasion by the fungus (positivity 6 h post-infection) earlier than the use of cultures (positivity only 24 h post-infection) (Costa et al., 2018). Given the advantages of nuclear techniques for studying fungal pathogenesis, our goal was to standardize the conditions for radiolabeling *C. albicans* with $^{99\ m}$Tc and use this microorganism as a model to study the effects of fecal material on the prognosis of IAC.

2. Material and Methods

2.1. Reagents

Nystatin (Fragon, São Paulo, SP, Brazil), miconazole (Pharma Nostra, Rio de Janeiro, RJ, Brazil), fluconazole (Sigma-Aldrich, San Francisco, CA, USA), itraconazole (Prati-Donaduzzi, Toledo, PR, Brazil), crystal violet, 95 % ethanol, sodium chloride (NaCl), glutaraldehyde (Synth, São Paulo, SP, Brazil), stannous chloride dihydrate ($SnCl_2{\cdot}H_2O$) (Sigma-Aldrich, Frankfurt, HE, Germany), fetal bovine serum (Gibco, ThermoFisher Scientific, Los Angeles, CA, USA), and glucose (Inlab, São Paulo, SP, Brazil) were purchased from commercial suppliers and used without additional purification. Sabouraud-dextrose broth (SDB) and sabouraud-dextrose agar (SDA) were purchased from Kasvi (São José do Pinhais, PR, Brazil). Sodium pertechnetate ($Na^{99\ m}TcO_4$) was obtained by elution from a ^{99}Mo/$^{99\ m}$Tc generator (Ipen, São Paulo, SP, Brazil) with sterile saline solution.

Polyvinyl chloride (PVC) urethral catheters (Embramed®; São Paulo, SP, Brazil) were obtained from stores specialized in hospital-medical supplies.

2.2. Microorganism

C. albicans SC5314 (ATCC MYA-2876) was used in this study. This strain is originated from the American Type Culture Collection (ATCC) and was kindly provided by the Reference Microorganisms Laboratory of the Oswaldo Cruz Foundation (FIOCRUZ; Rio de Janeiro, RJ, Brazil). The yeast was cultured on SDA at 37 °C for 48 h prior to the tests. For all experiments, yeast cells were suspended in sterile saline pH 7 (NaCl 0.9 % w/v), and the inoculum was adjusted in a spectrophotometer to $\sim 10^7$ colony-forming units (CFU) per mL (optical density at 530 nm – $OD_{530\ nm}$: 0.700–0.800; Bio-Tek Instruments, New York, NY, USA).

2.3. Candida albicans radiolabelling

Initially, the best experimental conditions for radiolabeling of *C. albicans* with $^{99\ m}$Tc were determined. For this, the optimal concentration of the reducing agent ($SnCl_2.2H_2O$), which is necessary to reduce the $^{99\ m}TcO_4^-$ ion to lower oxidation states, making it reactive, and the suitable incubation time were investigated. Briefly, yeast suspensions at $\sim 10^7$ CFU/mL in triplicate were incubated with variable concentrations of $SnCl_2.2\ H_2O$ (0, 50, 100, 150, and 200 μM in 0.25 N HCl) for 10 min at 37 °C. Then, 18.5 MBq (500 μCi) of $Na^{99\ m}TcO_4$ was added to the solution, followed by incubation at 37 °C for 10, 20, or 30 min and centrifugation at 3000 *g* for 25 min (CralTech, Cotia, SP, Brazil). Further, 100 μL of the supernatant was collected, and the rest discarded. One mL of sterile saline was added to the pellet, which was homogenized, and 100 μL was collected. The radioactivity of the supernatant and precipitate was determined by Wizard Gama Counter (Perkin-Elmer, Turku, Finland), and the procedure was repeated twice. Finally, the percentage of $^{99\ m}$Tc incorporated into the fungal cells (precipitate) was determined from values of counts per minute (CPM) using the Eq. 1:

$$\%\ ^{99\ m}\text{Tc-}\textit{Candida albicans} = [\text{CPM (Precipitate)/CPM (Precipitate+Supernatant)}]\ \text{x}\ 100 \quad (1)$$

2.4. $^{99\ m}$Tc-Candida albicans stability

The stability of the $^{99\ m}$Tc-*C. albicans* complex was investigated by incubation of the radiolabeled microorganism at 37 °C in saline for 0, 24, 36, 48, 60, e 72 h, followed by the determination of the percentage of radiolabeling at each time interval (Eq. 1) (Costa et al., 2018; Diniz et al., 1999).

2.5. Fungal viability of $^{99\ m}$Tc-Candida albicans

2.5.1. Viable cell load

The number of viable cells was determined to investigate the impact of radiolabeling on the viability of *C. albicans* (Costa et al., 2018). Briefly, aliquots (100 μL) were taken from the fungal suspensions after the last wash, serially diluted in sterile saline (10^{-1}–10^{-6}), spread into the surface of a solid culture medium (SDA) and incubated at 35 ± 2 °C for 48 h. Then, the colonies were counted, and the results were expressed as CFU/mL. The fungal load of radiolabeling cells was compared to unlabeled *C. albicans*.

2.5.2. Growth curve

A growth curve assay was performed to assess the radiolabeling effects on the viability of *C. albicans* in the function of time (Machuca et al., 2016). Aliquots of 100 μL of the radiolabeled yeast suspension at $\sim 10^7$ CFU/mL were added to wells containing 100 μL of SDB. The plates were incubated at 35 ± 2 °C for 48 h, and the optical density (OD) at 600 nm was determined in several time intervals (1, 2, 3, 4, 5, 6, 24, and 48 h) using a microplate reader (Bio-Tek Instruments, New York, NY, USA). Finally, the results of the growth curve of radiolabeling yeast were

graphically expressed as a function of $OD_{600\ nm}$ vs. incubation time and compared to the growth curve of unlabeled cells.

2.6. Structural analysis of $^{99\ m}$Tc-Candida albicans

Fungal cell structure after radiolabeling was evaluated by light microscopy and scanning electron microscopy.

2.6.1. Gram staining

Light microscopy analysis was performed in cells stained with the Gram technique. A suspension of technetium-labeled cells was centrifuged and the precipitate fixed on a glass slide with heat. After fixation, the material was exposed to crystal violet (1 min), lugol (1 min), absolute alcohol (0.5 min), and fuchsin (1 min). The slides were washed with running water between each staining step. After the procedure, the slides were evaluated under optical microscopy (Nikon TE 2000-U Eclipse, Tokyo, Japan) at 1000x magnification. The structure of the labeled cells was visually compared to the structure of the unlabeled yeast.

2.6.2. Scanning electronic microscope

One milliliter (1 mL) of a suspension of $^{99\ m}$Tc-radiolabeled and non-radiolabeled *C. albicans* was diluted in sterile saline and centrifuged at 12,000 *g* for 5 min. The pellet was resuspended in 1 mL of saline and centrifuged. Next, 15 μL of cell suspension was added to an aluminum stub and allowed to wet at 37 °C for 30 min. Then, the yeasts were fixed with a solution containing 2.5 % (v/v) glutaraldehyde for 3 h at room temperature. The material was dehydrated in a graded ethanol series (70 %, 90 %, and 100 % v/v; 30 min in each solution), and the samples were dried in a desiccator containing silica gel overnight. The stubs were coated by sputtering with a 10 nm layer of gold and visualized using a scanning electron microscope (Jeol JSM-6010Plus/LA®, Zeiss®, Oberkochen, West Germany).

2.7. $^{99\ m}$Tc-Candida albicans biofilm formation

2.7.1. Microplate assay

The effect of radiolabeling on the biofilm formation of *C. albicans* was evaluated by the crystal violet method (Andrade et al., 2021). A yeast suspension with a cell density of $\sim 10^7$ CFU/mL was prepared in sterile saline using radiolabeled or non-radiolabeled cells. Then, 100 μL was transferred to 10 mL of SDB supplemented with 100 mM glucose. 100 μL of the resulting suspension was pipetted into sterile 96-well microplates, which were incubated at 37 °C for 24, 48, and 72 h to allow biofilm formation. After the incubation period, the biofilms were revelated with 0.1 % w/v crystal violet solution, diluted with absolute ethanol, and the $OD_{595\ nm}$ of wells was determined in a microplate reader (Bio-Tek Instruments, New York, NY, USA).

2.7.2. Urethral catheter assay

Biofilm formation on sterile catheter segments was conducted according to Sousa et al. (2019) One centimeter (1 cm) sterile PVC urethral catheter segments were immersed in tubes containing a radiolabeling or non-radiolabeling *C. albicans* suspension at $\sim 10^7$ CFU/mL in SDB supplemented with 100 mM glucose. The tubes were incubated at 35 ± 2 °C for 48 h to allow biofilm formation on the catheter surface. Then, the yeast cultures were discarded, and the catheter segments were transferred to tubes with 5 mL of sterile saline and remained under shaking for 30 min. The segments were removed with sterilized dissection forceps, transferred to another tube containing 5 mL of sterile saline, and sonicated for 5 min at 40 KHz (Soniclean, New York, NY, USA). The samples were then homogenized, and 100 μL aliquots were serially diluted (10^{-1} –10^{-6}) in sterile saline and plated onto SDA. The plates were incubated at 35 ± 2 °C for 48 h, and the CFU/cm of the catheter was determined by colony counting.

2.8. Yeast-to-Hyphae transition of $^{99\ m}$Tc-Candida albicans

The effect of radiolabeling on the yeast-to-hypha transition of *C. albicans* was also evaluated. Hyphae induction was conducted by incubating radiolabeled and non-radiolabeled *C. albicans* in microplates containing FBS at 50 % v/v. Posteriorly, the microplates were incubated for 24, 48, and 72 h at 35 ± 2 °C, and the hypha formation was observed by a light microscope (Nikon TE 2000-U Eclipse, Tokyo, Japan) with a magnification of 400× (Andrade et al., 2021).

2.9. Antifungal susceptibility

To assess whether radiolabeling alters the susceptibility of *C. albicans* to antifungal agents, the activity of four compounds (i.e., nystatin, miconazole, fluconazole, and itraconazole) was determined by the broth microdilution method, as described by the document M27-A2 of the Clinical Laboratory Standard Institute (CLSI) (Clinical and Laboratory Standards Institute, 2017). The antifungals were two-fold serial diluted (0.5–32 μg/mL) in microplates containing SDB. Subsequently, 100 μL of a radiolabeling or non-radiolabeling *C. albicans* inoculum ($\sim 10^3$ CFU/mL) prepared in sterile saline were added to each well. The plates were incubated at 35 ± 2 °C for 48 h, and the minimum inhibitory concentration (MIC) of the compounds was defined as the lowest concentration of antifungals that inhibited the visible growth of the yeast (Andrade et al., 2021).

2.10. In vivo assay

2.10.1. Animals

Female Swiss mice (6–8 weeks old) were housed under specific pathogen-free (SPF) conditions in polyethylene cages with eight mice per cage, at a temperature of 25 ± 2 °C, a light-dark cycle of 12/12 h, and received water and commercial food (Nuvilab®, Colombo, PR, Brazil) ad libitum. All experimental protocols rigorously followed the international norms of animal management, and the protocols were approved by the Animal Experimentation Ethics Committee of the Universidade Federal de Minas Gerais (Protocol 121/2021).

2.10.2. Intra-abdominal candidiasis induction

An IAC model was induced in immunosuppressed mice according to Lima et al. (2019), with modifications. Mice received an intraperitoneal (i.p.) injection of dexamethasone (Teuto, Curitiba, PR, Brazil) at 10 mg/Kg/day for nine consecutive days. On the seventh day, the animals were infected by intraperitoneal injection with 0.2 mL of $^{99\ m}$Tc-*C. albicans* suspension ($\sim 10^7$ cells/mL) prepared in sterile saline with (n = 15) or without (n = 15) mouse feces. Feces from uninfected mice were ground in a tissue grinder, suspended in normal saline to form a 5 % weight/volume mixture, and sterilized in a steam autoclave (15 min, 200 kPa, 120 °C) (Cheng et al., 2013). IAC was confirmed by peritoneal lavage culture, which has a maximum fungal load 48 h post-infection (Lima et al., 2019, 2021).

2.10.3. Biodistribution of $^{99\ m}$Tc-C. albicans

The biodistribution assay was performed to test the dynamics of the distribution of $^{99\ m}$Tc-*C. albicans* in mice after IAC with and without fecal material. After 24, 48, and 72 h of infection, the blood, brain, lungs, liver, spleen, heart, and stomach were collected, weighed, and the radioactivity was measured in a Wizard Gama Counter (Perkin-Elmer, Turku, Finland) (Costa et al., 2018). The results were expressed as the percentage of injected dose (%ID) by the weight (in g) of each tissue evaluated. To compare the performance of classic and nuclear methods, the fungal load in all tissues was also determined by plating on SDA supplemented with 0.05 % chloramphenicol. A semi-quantitative method was used in the culture assay, with the fungal load defined as Absent (0), when no visible colonies were detected in the culture medium; Low (1), when less than 10 colonies were identified in the culture

medium; Moderate (2), when 10–100 colonies were identified in the culture medium; and High (3), when more than 100 colonies were identified.

2.11. Statistical analysis

All in vitro experiments were performed in triplicate in different days, with three replicates in each test. Data normality was confirmed by the Shapiro-Wilk test and represented as the mean±standard deviation, when necessary. The in vitro assays were evaluated by One-Way ANOVA followed by Tukey's or Dunnett post-test to multiple comparations or Studentś t-test for comparations between two groups. For the Dunnett post-test, the saline group was used as the control group in all analyses. The data from the in vivo experiments showed non-gaussian distribution in the Shapiro-wilk test, and the results were expressed as the median and interquartile range when necessary. The differences in the biodistribution assay and the fungal load in tissues of mice infected with fecal material and mice infected without fecal material were determined by the Mann-Whitney test. All statistical analyses were assessed using GraphPad Prism 5.03 (GraphPad Software Inc., LaJolla, CA), and p values < 0.05 were considered statistically significant.

3. Results

3.1. Standardization of radiolabelling conditions

Initially, the conditions for the radiolabeling procedure of *C. albicans* with $^{99\ m}$Tc were optimized. As shown in Table 1, 100 μM of the reducing agent $SnCl_2.2\ H_2O$ was the lowest concentration that showed higher labeling efficiency before washing (84.11 ± 1.79 %). Therefore, it was used as the standard conditions for further studies. Regarding the incubation time with the radionuclide, no difference was observed between the studied intervals (10, 30, and 60 min) (Table 2), and 10 min was chosen as the standard incubation time. In conclusion, incubation of *C. albicans* with 100 μM $SnCl_2.2\ H_2O$ for 10 min at 37 °C, followed by the addition of 18.5 MBq $^{99\ m}$Tc, ensured an efficient labeling of yeast greater than 99% after two washes with saline. Therefore, these conditions were standardized and used in subsequent analyses.

3.2. Stability of $^{99\ m}$Tc-Candida albicans

As shown in Table 3, the binding of technetium-99 m to *C. albicans* cells was significantly stable. Even after 72 h, a labeling efficiency of more than 99 % was observed.

3.3. Viability of $^{99\ m}$Tc-Candida albicans

The viability of *C. albicans* was assessed using the radiolabeling protocol with $^{99\ m}$Tc. First, the fungal load was determined using the limited dilution method. This assay showed that only the cells exposed to the reducing agent ($SnCl_2.2\ H_2O$) alone presented impaired cell viability (Fig. 1A). Then, the growth curve assay was performed to check the effect of radiolabeling procedures as a function of time. As shown in Fig. 1B, there was no statistical difference in the growth of the labeled fungal cells compared to unlabeled cells over 48 h. Only *C. albicans* exposed to the reducing agent ($SnCl_2.2H_2O$) showed decreased growth ($OD_{600\ nm}$ after 48 h: $SnCl_2.2\ H_2O$: 0.26 ± 0.03 vs. saline: 1.21 ± 0.7; $p<0.0001$).

Table 1
Effect of different concentrations of the reducing agent ($SnCl_2.2H_2O$) on the labeling efficiency of *Candida albicans* with technetium-99 m.

$SnCl_2.2H_2O$ (μM)	% of radioactivity in *Candida albicans*		
	Before the washes	After the washes	
		1	2
0	6.41 ± 1.28[a]	3.98 ± 1.30[a]	9.26 ± 1.10[a]
50	69.80 ± 10.99[b]	98.55 ± 0.19[b]	99.38 ± 0.29[b]
100	84.11 ± 1.79[b,c]	99.13 ± 0.35[c]	99.36 ± 0.14[b]
150	94.15 ± 5.41[c]	98.12 ± 1.74[b,c]	99.38 ± 0.16[b]
200	91.57 ± 5.01[c]	99.55 ± 0.23[c]	99.51 ± 0.26[b]

Data normality was confirmed by the Shapiro-Wilk test. Analysis of variance (ANOVA) followed by Tukey's post-test was performed. Different letters represent statistically relevant differences (p-value<0.05)

Table 2
Influence of incubation time on the yield of *Candida albicans* labeling with technetium-99 m.

Time (min)	% of radioactivity in *Candida albicans*		
	Before the washes	Before the washes	
		1	2
10	82.01 ± 10.30[a]	99.05 ± 0.84[a]	99.47 ± 0.14[a]
30	82.03 ± 7.12[a]	98.90 ± 0.63[a]	99.60 ± 0.12[a]
60	89.04 ± 8.28[a]	99.57 ± 0.17[a]	99.67 ± 0.08[a]

For the execution of the present test, a solution of stannous chloride (SnCl2.2H2O) at 100 μM was used. Data normality was confirmed by the Shapiro-Wilk test. Analysis of variance (ANOVA) followed by Tukey's post-test was performed. Different letters represent statistically relevant differences (p-value <0.05)

Table 3
Stability of *Candida albicans* radiolabelled with 99 m-technetium.

Time (h)	% of radioactivity in *C. albicans*
0	99.37 ± 0.23[a]
24	99.98 ± 0.01[a]
36	99.96 ± 0.03[a]
48	99.39 ± 0.46[a]
60	98.90 ± 0.79[a]
72	99.46 ± 0.16[a]

Data normality was confirmed by the Shapiro-Wilk test. Analysis of variance (ANOVA) followed by Tukey's post-test was performed. Equal letters represent statistically non relevant differences (p-value > 0.05)

3.4. Cellular morphology of $^{99\ m}$Tc-Candida albicans

To examine whether the incorporation of $^{99\ m}$Tc into the cell structure of *C. albicans* affects its morphology, we analyzed labeled and unlabeled cells by light microscopy and scanning electron microscopy (SEM). Gram staining showed that radiolabeling does not alter *C. albicans* morphology, as both cells are oval and purple-stained (purple crystal is preserved) (Fig. 2). A large amount of eosinophilic material was detected in the cells labeled with $^{99\ m}$Tc, possibly due to the presence of the reducing agent ($SnCl_2.2\ H_2O$) that usually precipitates after oxidation by the technetium. SEM analyses (Fig. 2) confirmed the Gram staining results and demonstrated that the ultracellular structure of *C. albicans* remains unchanged after radiolabeling.

3.5. Biofilm formation ability by $^{99\ m}$Tc-Candida albicans

One of the most important virulence factors of *C. albicans* that affects human health is the ability of this pathogen to form biofilms. To test whether radiolabeling with $^{99\ m}$Tc affects the ability of this yeast to form biofilms, we examined the amount of biofilm formed using the crystal violet assay. As shown in Fig. 3, radiolabeling does not alter the amount of biofilm formed after 24 and 48 h of incubation compared to unlabeled cells. Interestingly, the cells exposed only to the reducing agent ($SnCl_2.2\ H_2O$) formed an increased amount of biofilms after 24 and 48 h compared to the unexposed cells. However, after 72 h of incubation, when the biofilm reaches its greatest biomass, the cells exposed to $^{99\ m}$Tc

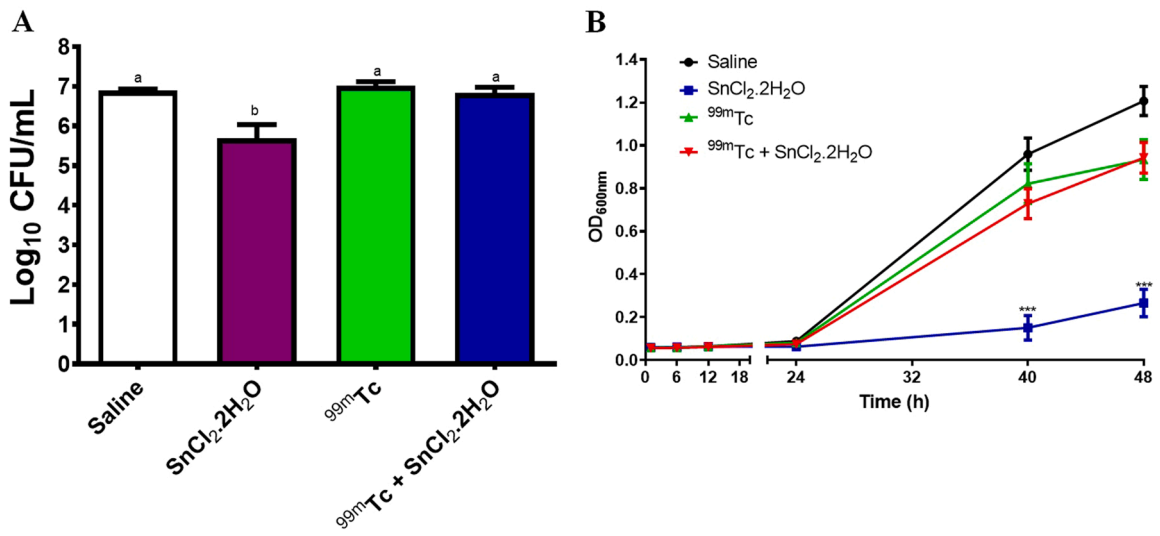

Fig. 1. Determination of the viability of $^{99\,m}$Tc-*Candida albicans*. A - Evaluation of the fungal load by the limiting dilution assay of a suspension of *C. albicans* exposed to different conditions used for radiolabeling of yeasts with technetium-99 m. Different letters represent statistically relevant differences (p-value <0.05). This experiment was analyzed by One-way ANOVA with Tukey's post-hoc test. B - Growth curve over 48 h of *C. albicans* exposed to different conditions used for radiolabeling of yeasts with technetium-99 m. Three asterisks (***) indicate statistically different compared to the saline group with $p < 0.0001$. This experiment was analyzed by One-way ANOVA with Dunnett post-hoc.

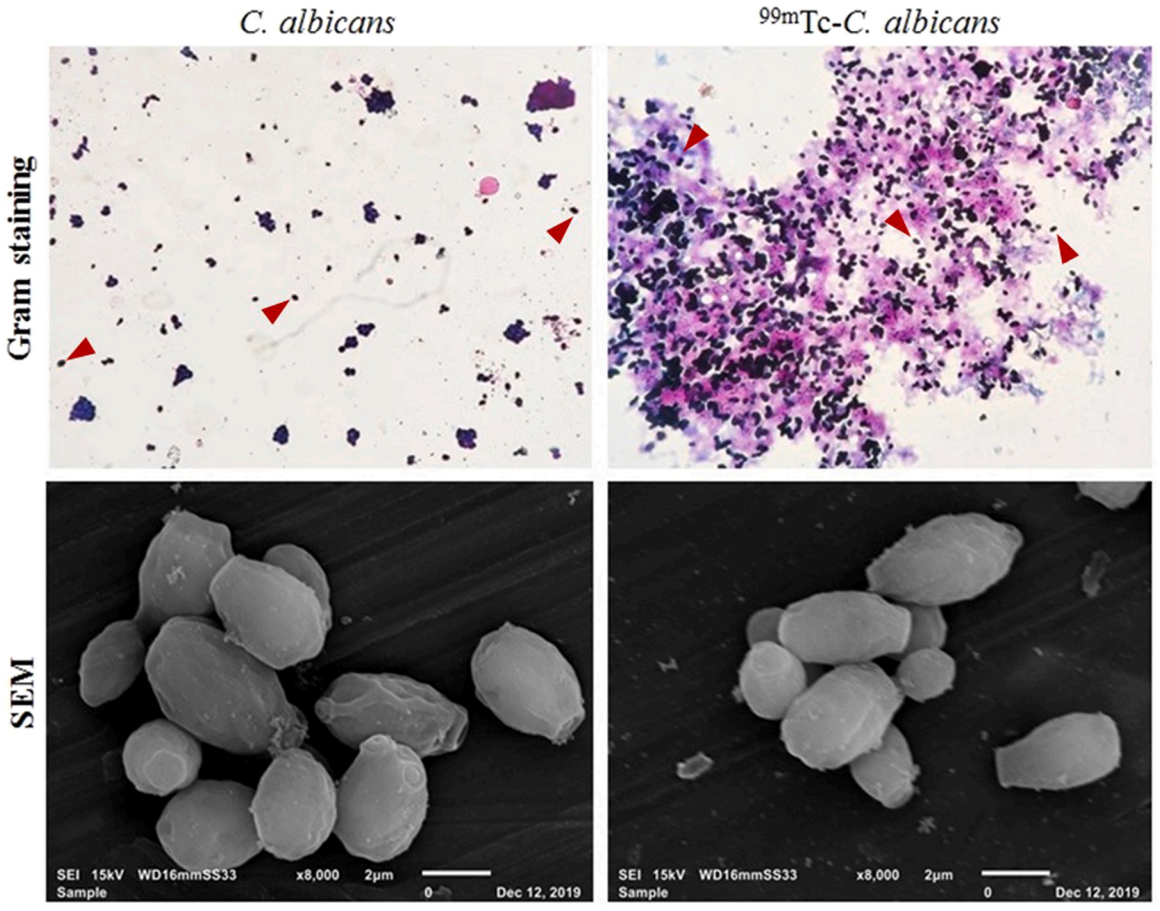

Fig. 2. Cell structure of *Candida albicans* labeled and unlabeled with technetium-99 m analyzed by light microscopy after Gram staining and scanning electron microscopy.

have a significantly lower amount of biofilm than the non-exposed cells (Fig. 3C). Confirming these results, the determination of fungal load in biofilms established in a bladder catheter showed significantly lower cell density for $^{99\,m}$Tc-*C. albicans* (*C. albicans*: 5.987 ± 0.09 Log_{10} CFU/cm vs. $^{99\,m}$Tc-*C. albicans*: 4.758 ± 0.23 Log_{10}CFU/cm; $p < 0.0001$) (Fig. 4), suggesting that gamma radiation emitted by technetium impairs the

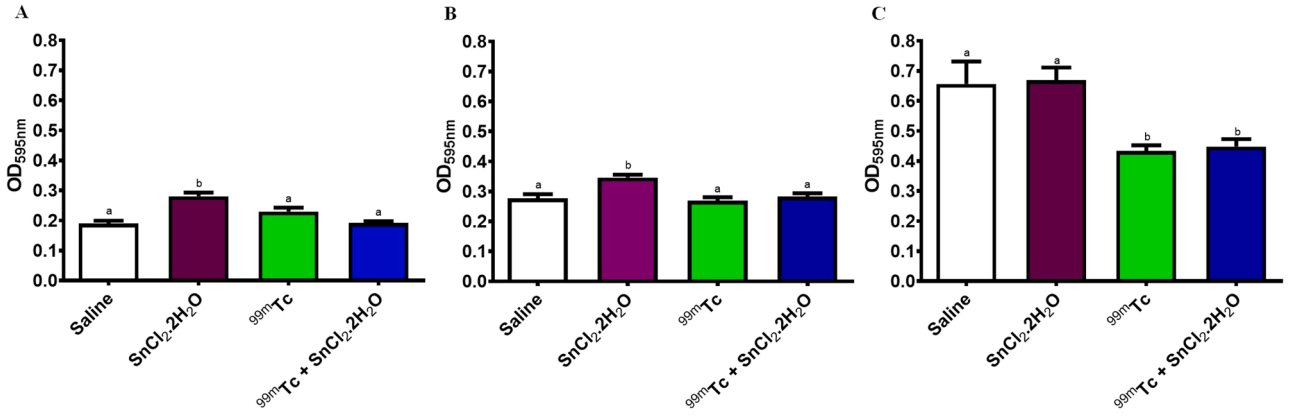

Fig. 3. Biofilm biomass formed by *Candida albicans* exposed to different conditions used for radiolabeling of yeasts with technetium-99 m after 24 h (A), 48 h (B) and 72 h (C) of incubation at 35 ± 2 °C. Different letters represent statistically relevant differences compared to the saline group (p-value <0.05). This experiment was analyzed by One-way ANOVA with Tukey's post-hoc test.

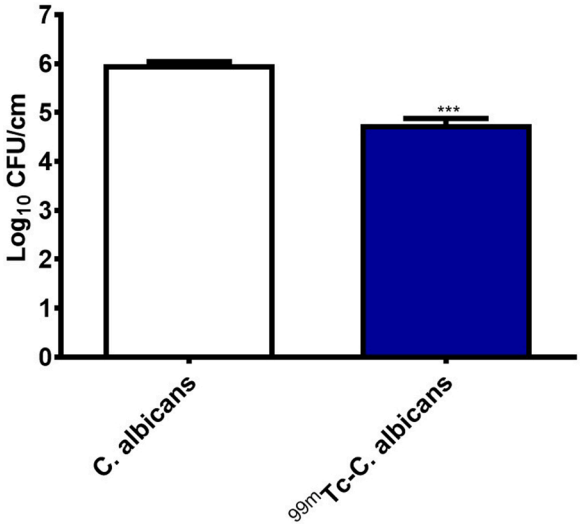

Fig. 4. Fungal load of *Candida albicans* and $^{99\,m}$Tc-*Candida albicans* biofilms formed on the surface of a PVC urethral catheter. Three asterisks (***) indicate statistically different compared to the saline group with $p < 0.0001$. This experiment was analyzed by Student's t-test.

ability of *C. albicans* to form biofilms.

3.6. Filamentation of $^{99\,m}$Tc-Candida albicans

C. albicans is a dimorphic fungus that can be found as oval yeast cells or elongated hyphae. It is more virulent in the hyphal form and is commonly associated with superficial and systemic infections. To determine whether labeling with $^{99\,m}$Tc affects the ability of *C. albicans* to transition from yeast to hyphae, we examined the filament formation induced by fetal bovine serum. As shown in Fig. 5, radiolabeling did not affect the ability of *C. albicans* to form true hyphae, and the morphological transition was observed in all groups studied and at all times. Interestingly, the number of hyphae in the first 48 h was higher in cells exposed only to the reducing agent ($SnCl_2 \cdot H_2O$), confirming the results of the biofilm assay (Figs. 3A and B).

3.7. Susceptibility of $^{99\,m}$Tc-Candida albicans to antifungal agents

The antifungal activity of azoles (miconazole, itraconazole, and fluconazole) and the polyene nystatin was determined against labeled and unlabeled cells to determine whether technetium-99 m binding alters *C. albicans* susceptibility. Table 4 shows that the MICs of the antifungal agents were not altered by $^{99\,m}$Tc radiolabeling.

3.8. Use of $^{99\,m}$Tc-Candida albicans in a murine IAC model

To test the feasibility of using $^{99\,m}$Tc-*Candida albicans* as a model to study aspects of the pathophysiology of invasive infections, an IAC model was performed, and the biodistribution of this microorganism was determined after i.p. injection with and without mouse feces using nuclear techniques. As shown in Fig. 6, the biodistribution assay revealed that the spleen was the main target organ of IAC and the presence of fecal material affected the spread of *C. albicans* in this organ after 24 h (without mouse feces: 1.39 (0.59–2.16) vs. with mouse feces: 0.45 (0.32–0.47)), 48 h (without mouse feces: 5.34 (4.34–6.64) vs. with mouse feces: 0.31 (0.29–0.33), and 72 h (without mouse feces: 1.65 (1.44–1.81) vs. with mouse feces: 0.77 (0.54–1.40) of infection. Furthermore, there was a significant difference in the amount of $^{99\,m}$Tc-*C. albicans* in the liver, kidney, stomach, and heart of animals with fecal-induced IAC at 48 h post-infection, but not at 24 and 72 h, compared to mice that received the pathogen diluted in saline. Interestingly, a low radioactivity uptake was detected in the blood of both groups of animals (i.e., with and without fecal material) at the first time points evaluated (24 and 48 h), suggesting that the hematogenous route is not the most important for the spread of the pathogen during IAC. However, after 72 h, there was a significant increase in radioactivity uptake in the blood, heart, and brain, which could be related to the systemic impairment of the animals.

3.9. Culture and determination of fungal load

Organs and tissues removed from animals with IAC were macerated and seeded in SDA to assess the fungal load by classical methods. Table 5 shows that the behavior observed in the biodistribution test was consistent with the microbiological findings in culture. Animals with IAC induced in the absence of fecal material had higher fungal loads in the spleen at all intervals evaluated (24, 48, and 72 h), similar to what was observed in the biodistribution test. Moreover, no viable fungal cells were recovered from the blood after 24 and 48 h of incubation, indicating low hematogenous dissemination, as observed in the biodistribution study. The brain was the least affected organ by infection, confirmed by the %ID/g data.

4. Discussion

Technetium-99 m is an artificial radionuclide obtained in generators by the decay of molybdenum-99 (^{99}Mo) (Payolla et al., 2019; Kane and

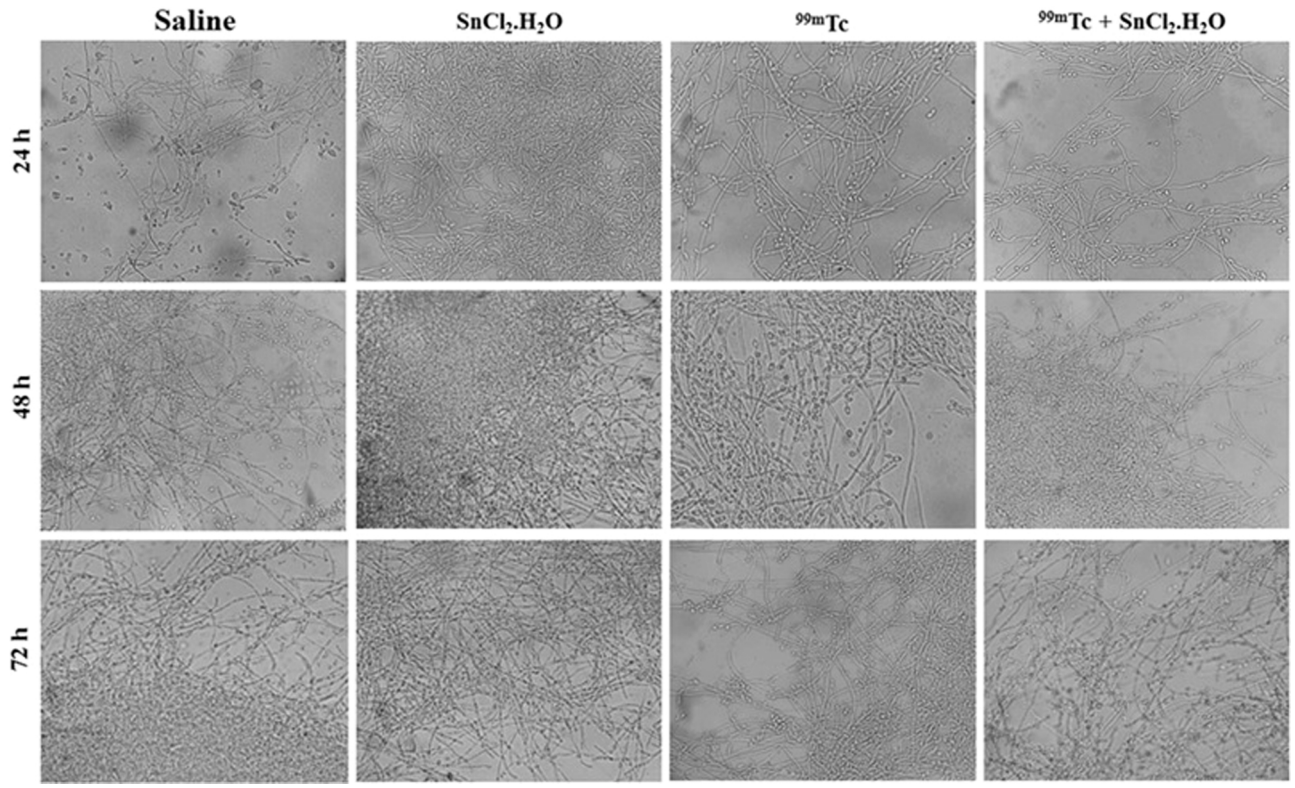

Fig. 5. Yeast-to-hypha transition of *Candida albicans* cells exposed to different conditions employed in radiolabeling of yeasts with technetium-99 m.

Table 4
Minimum inhibitory concentration (MIC) of antifungals against $^{99\,m}$Tc-*Candida albicans*.

Antifungals	MIC (μg/mL)	
	C. albicans	$^{99\,m}$Tc-*C. albicans*
Fluconazole	2	2
Miconazole	2	2
Intraconazole	1	1
Nystatin	4	4

The isolate evaluated (Candida albicans SC5314) is sensitive to all antifungals tested according to the CLSI cut-off point (CLSI, 2017).

Davis, 2021). This radioactive element has several physicochemical properties compatible with its use in biological systems, such as reasonable half-life ($T_{1/2}$ = 6.01 h), emission of low-energy gamma radiation (140 keV), extraction in a portable generator, lack of volatility, and high reactivity with electron donor groups (e.g., -OH, -COOH, -NH2 and -SH) (Kane and Davis, 2021). These properties justify that $^{99\,m}$Tc is the most widely used radionuclide in nuclear medicine worldwide (Payolla et al., 2019; Wilhelm et al., 1999). Furthermore, $^{99\,m}$Tc has been successfully used to label microorganisms of medical interest, such as *E. coli* (Diniz et al., 1999) and *C. gattii,* (Costa et al., 2018) becoming the most suitable for radiolabeling *C. albicans*.

$^{99\,m}$Tc is obtained in the form of sodium pertechnetate (Na $^{99\,m}TcO_4$) in a ^{99}Mo/$^{99\,m}$Tc generator, which has low reactivity. Therefore, to obtain a good labeling yield, this nuclide must be reduced to lower oxidation states (Kane and Davis, 2021). Reducing agents such as stannous chloride dihydrate are used for this purpose. Determining the stannous chloride concentration required for radiolabeling with $^{99\,m}$Tc is performed empirically for each system and is not a trivial task when considering labeling microorganisms (Costa et al., 2018; Diniz et al., 1999). In fact, $SnCl_2.2H_2O$ is toxic and mutagenic in yeast cells. In the viability tests, we showed that stannous chloride reduces fungal load and significantly impairs the replication of *C. albicans* (Fig. 1). Viau (2005) confirmed our results and showed that stannous chloride has toxic potential and significant mutagenic activity in various reversion tests with *Saccharomyces cerevisiae*. The study indicates that DNA damage is caused by reactive oxygen species generated by exposure to this reducing agent (Viau, 2005). Interestingly, stannous chloride loses its antimicrobial capacity after the addition of $^{99\,m}$Tc. This can be justified by the fact that stannous chloride is oxidized to the Sn^{+4} state in the presence of the radionuclide and thus loses its ability to induce mutagenesis and other toxic effects in the fungal cell (Kane and Davis, 2021; Viau, 2005).

In order to determine the optimal amount of $SnCl_2.2H_2O$ that induces the reduction of $^{99\,m}$Tc without affecting the viability of the yeast, we tested different concentrations of this agent. We showed that $SnCl_2.2H_2O$ at 100–200 μM (Table 1) has the highest efficiency for radiolabeling. As for the incubation time with the radionuclide ($^{99\,m}$Tc), a period of 10 min showed the best labeling yield. Similar results were reported by Diniz et al. (1999), who obtained more than 90 % labeling efficiency for *E. coli* by using $SnCl_2.2H_2O$ at 100 μM followed by incubation with $^{99\,m}$Tc for 10 min

The binding of *C. albicans* with $^{99\,m}$Tc was stable for up to 72 h in this study. Similar results were obtained for radiolabeling of *C. gattii* (Costa et al., 2018) and *E. coli* (Diniz et al., 1999) with $^{99\,m}$Tc, demonstrating stability for 24 and 36 h, respectively. Moreover, no change in cell viability or structure was observed after radiolabeling of *C. albicans*, which was also reported for other microorganisms (Costa et al., 2018; Diniz et al., 1999). Therefore, these results confirm the success of radiolabeling *C. albicans* with $^{99\,m}$Tc.

The virulence of *C. albicans* warrants its adaptability to a wide variety of environments, making this pathogen capable of infecting virtually any part of the human body (Staniszewska, 2020). For $^{99\,m}$Tc-*C. albicans* to be used as a novel model to study invasive fungal infections, radionuclide binding should not affect the virulence of the pathogen. Although radiolabeling resulted in a reduction in the ability of *C. albicans* to form biofilms, no impairment of the inherent filamentous capacity of this pathogen was observed. The observation that *C. albicans*

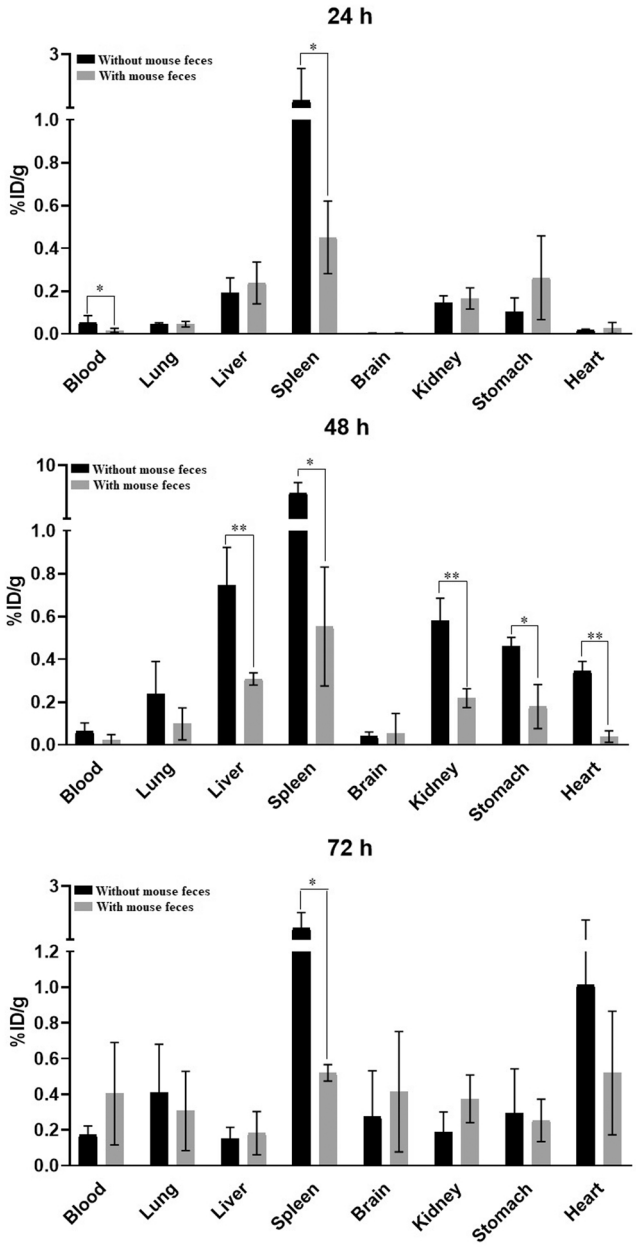

Fig. 6. Biodistribution of ^{99m}Tc-*Candida albicans* after intraperitoneal injection with and without mouse feces. The data show the percentage of injected dose per gram of organ (%ID/g) after 24, 48, and 72 h of infection. The data presented a non-Gaussian distribution as indicated by the Shapiro-Wilk test. The results of each organ were compared using the Mann-Whitney test, and all values were expressed as the median and interquartile range (Percentile 25-Percentile 75). One asterisk (*) indicates statistically different with $p < 0.05$. Two asterisks (**) indicate statistically different with $p < 0.001$.

is predominantly present in the hyphal form in the bloodstream and peritoneal fluid of patients with candidiasis suggests that the transition from yeast-to-hyphae is crucial for invasive infections (Centers for Disease Control and Prevention, 2020; Staniszewska, 2020). The establishment of candidemia in IAC, for example, is mainly related to the enhanced ability of hyphae to penetrate the peritoneum and underlying tissues and enter the bloodstream (Azim et al., 2017; Vergidis et al., 2016). In addition, phagosome hyphal formation has been shown to contribute to the ability of *C. albicans* cells to evade phagocytosis and kill macrophages (Kornitzer, 2019). Therefore, the fact that radiolabeling maintains the ability of the yeast to form true hyphae, makes ^{99m}Tc-*C. albicans* a promising tool for studying factors related to host-parasite interactions in invasive fungal infection models.

Another potential application of radiolabeled microorganisms is the evaluation of new experimental treatments or novel therapeutic protocols that combine conventional antifungal agents (Lima et al., 2021; Scorzoni et al., 2017). For ^{99m}Tc-*C. albicans* to be used for this purpose, the sensitivity of this pathogen must remain unchanged after radiolabeling. Our results show that ^{99m}Tc binding does not alter the sensitivity of *C. albicans* to azoles and polyenes. This justifies the use of this microorganism in studies aiming to investigate the pharmacological properties of antifungal agents.

After standardization and in vitro characterization of ^{99m}Tc-*C. albicans,* we used this microorganism to study relevant aspects of IAC. One of the least studied events of this infection is the role of fecal material in the development and prognosis of the disease. Therefore, we infected animals by i.p. injection with a suspension of ^{99m}Tc-*C. albicans* prepared in saline or a sterile mouse fecal solution. The biodistribution assay showed that the spleen and liver were the organs most affected by the infection, confirming previous studies (Andrade et al., 2021; Lima et al., 2019). Because they are components of the reticuloendothelial system, the liver and spleen have a high density of resident immune cells and are involved in the clearance of infectious agents that manifest in invasive forms (Singh et al., 2020).

Notably, the fungal load in both assays (%ID/g and culture) was higher in animals receiving ^{99m}Tc-*C. albicans* without fecal material, suggesting that the presence of this component reduces the invasiveness of the pathogen. Previous studies showed that fecal material increases the formation of peritoneal abscesses in IAC models, whereas direct injection of *C. albicans* produces peritonitis with few abscesses (Cheng et al., 2014, 2013). The immune response involved in abscess formation provides efficient containment and subsequent elimination of the pathogen, thus impairing the invasion into extra-peritoneal organs (Cheng et al., 2013). In this context, our study confirmed this observation by showing that the concentration of fungal cells in organs of the abdominal cavity is significantly lower in animals exposed to fecal material, especially after 48 h of infection.

This study showed that the radiolabeling of *C. albicans* with technetium is a rapid, simple, and efficient method for investigating relevant aspects of invasive fungal infections. Radiolabeling with ^{99m}Tc was not only successfully performed but also did not affect the viability, susceptibility, and filamentation ability of *C. albicans*. Moreover, the use of ^{99m}Tc-*C. albicans* was able to elucidate aspects related to IAC, such as the importance of the presence of fecal material in pathogenesis. In this context, our study demonstrated that fecal material reduces the invasiveness of *C. albicans* after i.p. administration, probably by stimulating the formation of abscesses that control the spread of infection.

Ethical approval

All experimental protocols rigorously followed the international norms of animal management, and the protocols were approved by the Animal Experimentation Ethics Committee of the Universidade Federal de Minas Gerais (Protocol 121/2021).

Funding

Conselho Nacional de Desenvolvimento Científico e Tecnológico (CNPq), Cordenação de Aperfeiçoamento de Pessoal do N í vel Superior (CAPES), and Fundaç ão de Amparo à Pesquisa do Estado de Minas Gerais (FAPEMIG).

CRediT authorship contribution statement

Aline Beatriz do Couto-Campos and **William Gustavo Lima:** Conceptualization; Data curation; Formal analysis; Investigation; Methodology; Project administration; Software; Validation;

Table 5
Semi-quantitative determination of fungal load in mice organs with ^{99m}Tc-*Candida albicans*-induced intra-abdominal candidiasis with and without mouse feces.

Organ	Fungal burden					
	24 h		48 h		72 h	
	Without mouse feces	With mouse feces	Without mouse feces	With mouse feces	Without mouse feces	With mouse feces
Blood	0 (0–0)	0 (0–0)	0 (0–0)	0 (0–0)	1 (0–1)	0 (0–2)
Lung	1 (0–1)	2 (1–3)	2 (2–3)	1 (0–2)	2 (1–3)	2 (0–3)
Liver	1 (0.75–1.25)	2 (1–2)	1 (1–2)	2 (1–2)	0 (0–1)	1 (0–3)
Spleen	2 (2–2)*	1 (1–3)	1 (1–1)*	1 (0–1)	1 (0–1)*	0 (0–0)
Brain	0 (0–0)	1 (1–1)	0 (0–2)	0 (0–1)	0 (0–2)	0 (0–0)
Kidney	1 (0–2)	3 (1–3)	1 (0–1)	1 (0–1)	0 (0–1)	0 (0–2)
Stomach	2 (1–2)	3 (3–3)	3 (3–3)	3 (3–3)	3 (2–3)	3 (2–3)
Heart	0 (0–1)	1 (0–3)	2 (2–2)	2 (2–2)	2 (0–3)*	0 (0–0)

0: when no visible colonies were detected in the culture medium; 1: when less than 10 colonies were identified in the culture medium; 2: when 10–100 colonies were identified in the culture medium; 3: when more than 100 colonies were identified in the culture medium.
The data presented a non-Gaussian distribution as indicated by the Shapiro-Wilk test, and the results of each organ were compared using the Mann-Whitney test. One asterisks (*) indicate statistically different with $p < 0.05$.

Visualization; Roles/Writing - original draft; Writing - review & editing. **Júlio César Moreira Brito:** Formal analysis; Investigation; Methodology. **Valbert Nascimento Cardoso:** Funding acquisition; Writing - review & editing. **Simone Odília Antunes Fernandes:** Supervision; Writing - review & editing.

Conflict of Interest

All authors report that they do not have any conflicts of interest.

Acknowledgments

W.G.L. is grateful to Cordenação de Aperfeiçoamento de Pessoal do N í vel Superior (CAPES) for a Ph.D. fellowship, as well as Conselho Nacional de Desenvolvimento Científico e Tecnológico (CNPq), Fundaç ão de Amparo à Pesquisa do Estado de Minas Gerais (FAPEMIG), and Pro-Reitoria de Pesquisa of Universidade Federal de Minas Gerais (PRPq/UFMG).

References

Andrade, J.T., Lima, W.G., Sousa, J.F., Saldanha, A.A., Nívea Pereira De Sá, Morais, F.B., Prates Silva, M.K., Ribeiro Viana, G.H., Johann, S., Soares, A.C., Araújo, L.A., Antunes Fernandes, S.O., Cardoso, V.N., Siqueira Ferreira, J.M., 2021. Design, synthesis, and biodistribution studies of new analogues of marine alkaloids: potent in vitro and in vivo fungicidal agents against Candida spp. Eur. J. Med. Chem. 210, 113048 https://doi.org/10.1016/j.ejmech.2020.113048.

Ardehali, R., Mohammad, S.F., 1993. 111Indium labeling of microorganisms to facilitate the investigation of bacterial adhesion. J. Biomed. Mater. Res. 27, 269–275. https://doi.org/10.1002/JBM.820270217.

Azim, A., Ahmed, A., Baronia, A.K., Marak, R.S.K., Muzzafar, N., 2017. Intra-abdominal candidiasis. EMJ Nephrol. 5, 83–92.

Centers for Disease Control and Prevention, 2020. Invasive Candidiasis Statistic [WWW Document]. CDC. URL ⟨https://www.cdc.gov/fungal/diseases/candidiasis/invasive/statistics.html⟩ (accessed 9.21.21).

Cheng, S., Clancy, C.J., Xu, W., Schneider, F., Hao, B., Mitchell, A.P., Nguyen, M.H., 2013. Profiling of Candida albicans gene expression during intra-abdominal candidiasis identifies biologic processes involved in pathogenesis. J. Infect. Dis. 208, 1529–1537. https://doi.org/10.1093/INFDIS/JIT335.

Cheng, S., Clancy, C.J., Hartman, D.J., Hao, B., Hong Nguyen, M., 2014. Candida glabrata intra-abdominal candidiasis is characterized by persistence within the peritoneal cavity and abscesses. Infect. Immun. 82, 3015. https://doi.org/10.1128/IAI.00062-14.

Clinical and Laboratory Standards Institute, 2017. Reference Method for Broth Dilution Antifungal Susceptibility Testing of Yeasts, 4rd ed. ed. Wayne (P.A.).

Costa, M.C., Mata, L.M., Ribeiro, N.D.Q., Santos, A.P.N., Oliveira, L.V.N., Vilela, R.V.R., Cardoso, V.N., Fernandes, S.O.A., Santos, D.A., 2018. A new method for studying cryptococcosis in a murine model using 99mTc-Cryptococcus gattii. Med. Mycol. 56, 479–484. https://doi.org/10.1093/MMY/MYX060.

Diniz, S.O., Resende, B.M., Nunan, E.A., Simal, C.J., Cardoso, V.N., 1999. 99mTechnetium labelled Escherichia coli. Appl. Radiat. Isot. 51, 33–36.

Diniz, S.O.F., Siqueira, C.F., Nelson, D.L., Martin-Comin, J., Cardoso, V.N., 2005. Technetium-99m ceftizoxime kit preparation. Braz. Arch. Biol. Technol. 48, 89–96. https://doi.org/10.1590/S1516-89132005000700014.

Eaves-Pyles, T., Wong, H.R., Wesley Alexander, J., 2000. Sodium arsenite induces the stress response in the gut and decreases bacterial translocation in a burned mouse model with gut-derived sepsis. Shock 13, 314–319. https://doi.org/10.1097/00024382-200004000-00010.

Fakhim, H., Vaezi, A., Javidnia, J., Nasri, E., Mahdi, D., Diba, K., Badali, H., 2020. Candida africana vulvovaginitis: prevalence and geographical distribution. J. Mycol. Med. 30 (3), 100966 https://doi.org/10.1016/j.mycmed.2020.100966.

Ghorbani, A., Sadrzadeh, A., Habibi, E., Dadgar, K., Akbari, J., Moosazadeh, M., Hossein, B., Ahangarkani, F., Vaezi, A., 2018. Efficacy of *Camellia sinensis* extract against *Candida* species in patients with denture stomatitis. Curr. Med. Mycol. 4 (3), 15–18. https://doi.org/10.18502/cmm.4.3.174.

Kane, S.M., Davis, D.D., 2021. Technetium-99m. Pract. Otol. 64, 1271–1277. ⟨https://doi.org/10.5631/jibirin.64.10special_1271⟩.

Kornitzer, D., 2019. Regulation of candida albicans hyphal morphogenesis by endogenous signals. J. Fungi 5. https://doi.org/10.3390/JOF5010021.

Lima, W.G., Alves-Nascimento, L.A., Andrade, J.T., Vieira, L., de Azambuja Ribeiro, R.I. M., Thomé, R.G., dos Santos, H.B., Ferreira, J.M.S., Soares, A.C., 2019. Are the Statins promising antifungal agents against invasive candidiasis. Biomed. Pharmacother. 111, 270–281. https://doi.org/10.1016/j.biopha.2018.12.076.

Lima, W.G., de Brito, J.C.M., Cardoso, V.N., Fernandes, S.O.A., 2021. In-depth characterization of antibacterial activity of melittin against Staphylococcus aureus and use in a model of non-surgical MRSA-infected skin wounds. Eur. J. Pharm. Sci. 156 https://doi.org/10.1016/j.ejps.2020.105592.

Lima, W.G., Araújo, M.G.F., Brito, J.C.M., Castilho, R.O., Cardoso, V.N., Fernandes, S.O. A., 2022. Antifungal effect of hydroethanolic extract of Fridericia chica (Bonpl.) L. G. Lohmann leaves and its therapeutic use in a vulvovaginal candidosis model. J. Mycol. Med. 32 (3), 101255 https://doi.org/10.1016/j.mycmed.2022.101255.

Machuca, J., Ortiz, M., Recacha, E., Díaz-De-Alba, P., Docobo-Perez, F., Rodríguez-Martínez, J.-M., Pascual, Á., 2016. Impact of AAC(6′)-Ib-cr in combination with chromosomal-mediated mechanisms on clinical quinolone resistance in Escherichia coli. J. Antimicrob. Chemother. 71, 3066–3071. https://doi.org/10.1093/jac/dkw258.

Millsop, J.W., Fazel, N., 2016. Oral candidiasis. Clin. Dermatol. 34, 487–494. https://doi.org/10.1016/j.clindermatol.2016.02.022.

Montravers, P., Dupont, H., Eggimann, P., 2013. Intra-abdominal candidiasis: the guidelines-forgotten non-candidemic invasive candidiasis. Intensive Care Med. 39, 2226–2230. https://doi.org/10.1007/S00134-013-3134-2.

Payolla, F.B., Massabni, A.C., Orvig, C., 2019. Radiopharmaceuticals for diagnosis in nuclear medicine: a short review. Eclética Quím. 44, 11–19. https://doi.org/10.1007/s12350-016-0498-z.

Schmiedel, Y., Zimmerli, S., 2016. Common invasive fungal diseases: an overview of invasive candidiasis, aspergillosis, cryptococcosis, and Pneumocystis pneumonia. Swiss Med. Wkly. 146, w14281 https://doi.org/10.4414/smw.2016.14281.

Scorzoni, L., de Paula e Silva, A.C.A., Marcos, C.M., Assato, P.A., de Melo, W.C.M.A., de Oliveira, H.C., Costa-Orlandi, C.B., Mendes-Giannini, M.J.S., Fusco-Almeida, A.M., 2017. Antifungal therapy: new advances in the understanding and treatment of mycosis. Front. Microbiol. 08, 36. https://doi.org/10.3389/fmicb.2017.00036.

Singh, D.K., Tóth, R., Gácser, A., 2020. Mechanisms of pathogenic candida species to evade the host complement attack. Front. Cell. Infect. Microbiol. 10, 94. https://doi.org/10.3389/FCIMB.2020.00094/BIBTEX.

Sobel, J.D., 2007. Vulvovaginal candidosis. Lancet. https://doi.org/10.1016/S0140-6736(07)60917-9.

Sousa, J.K.T., Haddad, J.P.A., Oliveira, A.C., Vieira, C.D., Santos, S.G., 2019. In vitro activity of antimicrobial-impregnated catheters against biofilms formed by KPC-producing Klebsiella pneumoniae. J. Appl. Microbiol. 127, 1018–1027. https://doi.org/10.1111/jam.14372.

Staniszewska, M., 2020. Virulence factors in candida species. Curr. Protein Pept. Sci. 21, 313–323. https://doi.org/10.2174/1389203720666190722152415.

Vergidis, P., Clancy, C.J., Shields, R.K., Park, S.Y., Wildfeuer, B.N., Simmons, R.L., Nguyen, M.H., 2016. Intra-abdominal candidiasis: the importance of early source

control and antifungal treatment. PLOS One 11, 153247. https://doi.org/10.1371/JOURNAL.PONE.0153247.
Viau, C.M., 2005. Efeitos tóxicos e genotóxicos do cloreto de estanho (SnCl2) em bactéria e levedura. Universidade Federal do Rio Grande do Sul.
Wilhelm, A.J., Mijnhout, G.S., Franssen, E.J., 1999. Radiopharmaceuticals in sentinel lymph-node detection – an overview. Eur. J. Nucl. Med. 26, S36–S42.